

Crystalline Zwitterionic Stilbazolium Derivatives with Large Quadratic Optical Nonlinearities

Christophe Serbutoviez and Jean-François Nicoud*

*Institut de Physique et Chimie des Matériaux de Strasbourg, UM 380046,
CNRS-ULP-EHICS, Groupe des Matériaux Organiques, 23 rue du Loess, B.P. 20 CR,
F67037 Strasbourg Cedex, France*

Jean Fischer

*Laboratoire de Cristallochimie et de Chimie Structurale, UA CNRS 424, 4 rue Blaise Pascal,
F67070 Strasbourg Cedex, France*

Isabelle Ledoux and Joseph Zyss

*Centre National d'Etudes des Télécommunications, France Telecom, Laboratoire de Bagneux,
Centre Paris B, URA CNRS 250, 196 Avenue Henri Ravera F92220 Bagneux, France*

Received February 1, 1994. Revised Manuscript Received May 24, 1994*

The synthesis and quadratic nonlinear optical properties of a series of zwitterionic 4-substituted 4'-(*n*-sulfonatoalkyl)stilbazolium derivatives are described. The most active compounds in second harmonic generation (SHG) are obtained with the 3-sulfonatopropyl group. 4-Methylthio-4'-(3-sulfonatopropyl)stilbazolium, 4-*n*-butyl-4'-(3-sulfonatopropyl)stilbazolium and (3-sulfonatopropyl)stilbazolium (further called MTSPS, BPS, and SPS, respectively) were selected by the SHG powder test for further investigations. They present several crystal modifications depending on recrystallization conditions. MTSPS presents two highly SHG-active monohydrated crystalline phases, respectively, 2.4 and 1.3 times more than NPP in the Kurtz and Perry powder test at 1.06 μm . The single-crystal X-ray structure of the most active phase is presented. MTSPS·H₂O phase I crystallizes in the monoclinic space group $P2_1$, with two molecules per unit cell, with dimensions of $a = 10.380 \text{ \AA}$, $b = 11.124 \text{ \AA}$, $c = 6.968 \text{ \AA}$, $\beta = 99.93^\circ$. The conformation of the zwitterionic part of MTSPS molecule agrees well with molecular modeling calculations. The water molecule is involved in a hydrogen bond network linking the ribbonlike molecules along the c axis. In addition, within a sheet the hyperpolarizable chromophores are arranged so that an intermolecular charge transfer is possible. The electric-field-induced second-harmonic generation (EFISH) and ground-state dipole moment measurements of more soluble MTSPS and SPS analogs have been performed, leading for the first time to the hyperpolarizability β values of such zwitterionic species. Finally the quadratic nonlinear susceptibilities of MTSPS materials have been estimated by using the oriented gas model, giving values in reasonable agreement with the experimental ones deduced from semiquantitative SHG powder tests.

Introduction

For the past decades organic materials that show quadratic [$\chi^{(2)}$] nonlinear optical (NLO) properties have been studied widely due to their promising potential applications in optical signal processing.^{1,2} To be efficient these organic materials must reconcile a number of potentially conflicting requirements such as the absence of inversion center at both molecular and macroscopic levels, they have to be prepared with chromophores that exhibit a large molecular hyperpolarizability (β), and they must satisfy some kind of phase-matching properties. It is now well established that β is closely related to molecules

that have a highly polarizable dissymmetric π -electron cloud induced by donor-acceptor interactions across a conjugated system, but since nearly 70% of organic compounds crystallize in a centrosymmetric crystal class, the probability to obtain an efficient NLO-active crystalline material remains rather low from molecules having the required electronic structure.³ Some various strategies have been built to permit the control of the crystal packing. Among them, the attachment of an additional polar group to the hyperpolarizable molecule has been a very attractive method and has been fruitfully developed in the case of NPAN [*N*-(4-nitrophenyl)-*N*-(methylamino)acetonitrile], a relevant crystalline material for nonlinear optics.^{4,5} We decided to extend this approach to longer hyperpolarizable backbone, and we focused our attention on the study of NLO materials containing a stilbazolium cation as nonlinear chromophore. Several stilbazolium molecular salts

* Author for correspondence.

• Abstract published in *Advance ACS Abstracts*, August 15, 1994.

(1) (a) *Nonlinear Optical Properties of Organic Molecules and Crystals*; Chemla, D. S., Zyss, J., Eds.; Academic Press: Orlando, 1987; Vols. 1, 2, and references therein. (b) *Molecular Nonlinear Optics. Materials, Physics, and Devices*; Zyss, J., Ed., Academic Press, Boston, 1994.

(2) Nicoud, J. F.; Twieg, R. J. Design and Synthesis of Organic Molecular Compounds for Efficient Second Harmonic Generation. In *Nonlinear Optical Properties of Organic Molecules and Crystals*; Chemla, D. S., Zyss, J., Eds.; Academic Press: New York, 1987; Vol. I, pp 227-296.

(3) Mighell, A. D. *Acta Crystallogr.* **1983**, *A39*, 737.

(4) Barzoukas, M.; Josse, D.; Fremaux, P.; Zyss, J.; Nicoud, J. F.; Morley, J. O. *J. Opt. Soc. Am. B* **1987**, *4*, 977.

(5) Vidakovic, P. V.; Coquillay, M.; Salin, F. *J. Opt. Soc. Am. B*, **1987**, *6*, 998.

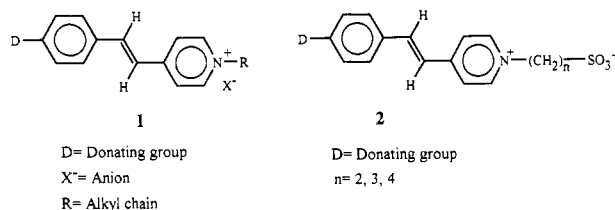


Figure 1. General structure of 4-substituted 4'-(*N*-alkyl)stilbazolium (1) and 4-substituted 4'-(*n*-sulfonatoalkyl)stilbazolium (2).

of type 1 (Figure 1; 1a D = N(CH₃)₂, R = CH₃, X⁻ = CH₃OSO₃⁻; 1b D = N(CH₃)₂, R = CH₃, X⁻ = TsO⁻) have been already reported to be highly efficient for second harmonic generation (SHG) by the SHG powder test.⁶⁻⁹ Unfortunately, first the growing of bulk single crystals of these organic salts seems rather problematic, and second, since they are ionic species the classical EFISH measurements cannot be performed so that very little was known in fact about their molecular hyperpolarizability β in solution.

Here we report on a new class of stilbazolium derivatives of type 2 (Figure 1), in which the anionic and the cationic parts are linked together by a *n*-alkyl chain, creating a large dipole moment that is independent of that due to the intramolecular charge transfer. These molecules are inner salts and belong to the family of zwitterions. [According to the IUPAC nomenclature, the name of these compounds is based on the selection of a parent ion in the molecule. Either ionic group can serve as the parent so that one can name compounds of type 2 by attaching the anionic sulfonatoalkyl chain to the stilbazolium cation or the cationic stilbazolium part to the anionic alkylsulfonate counterpart; in this paper we chose the former rule.] A wide range of these compounds has been synthesized by varying the donor groups and the length of the *n*-alkyl chains (*n* = 2, 3, 4). Among them, we have discovered two new organic crystals that exhibit efficient SHG powder tests and a favorable nonlinearity/transparency tradeoff. These new crystalline materials show polymorphism depending on the crystallization conditions. For one compound the crystal structure of two different SHG-active crystal modifications have been solved, one of them being reported here. For the first time, the EFISH measurements of the molecular hyperpolarizability of stilbazolium derivatives are reported showing the relevance of such zwitterionic molecules for the molecular design of new organic NLO materials.

Results and Discussions

Synthesis of New Materials. The preparation of 4-substituted 4'-(*n*-sulfonatoalkyl)stilbazolium derivatives 2 can be achieved by two different techniques, according to known procedures.¹⁰ The first one consists in the preparation of the stilbazole 3 by a direct synthesis of a carbon-carbon σ bond between 4-vinylpyridine 4 and a 4-substituted iodo- or bromobenzene 5 by a Heck type

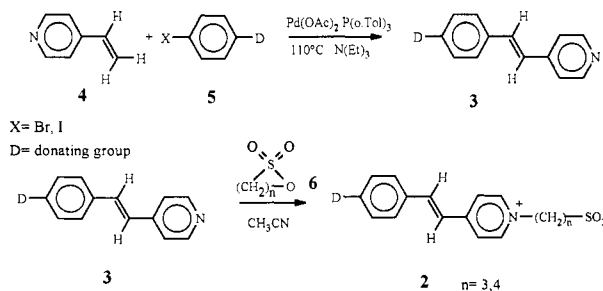


Figure 2. First way to synthesize 4-substituted 4'-(*n*-sulfonatoalkyl)stilbazolium (2, *n* = 3, 4).

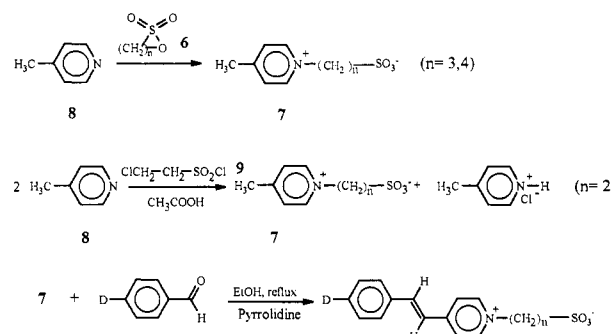


Figure 3. Second way to synthesize 4-substituted 4'-(*n*-sulfonatoalkyl)stilbazolium (2, *n* = 2, 3, and 4).

palladium-catalyzed coupling reaction.¹¹ The (*E*)-stilbazole 3 is then converted to 2 by reaction with a cyclic sultone 6 (Figure 2).

Following the second procedure (Figure 3), the zwitterionic derivative 7 is first prepared. For *n* = 3 or 4, 4-picoline 8 is reacted with the appropriate cyclic sultone, while for *n* = 2 the pyridinium derivative 7 is obtained by reaction of 8 with 2-chloroethanesulfonyl chloride 9 in acetic acid.¹² The methyl group in para position in 7 is activated enough for a base-catalyzed Knoevenagel condensation with a substituted benzaldehyde leading to the zwitterionic compound 2. This reaction afforded only the thermodynamically most stable (*E*)-2 isomer with moderate to good yields (50–90%).

In our hands, the second procedure appeared to be the most convenient, giving better yields. It was also the only way to prepare 4-substituted 4'-(2-sulfonatoethyl)stilbazolium derivatives (2, *n* = 2). The length variation of the alkyl chain between the pyridinium cation and the sulfonate anion was made to obtain some influence on the physical properties of the compounds (solubility in organic solvents, hydrophilicity, polarity, etc.). It also allowed the multiplication of the crystalline materials for NLO and might influence more or less strongly the crystal packing.

Quadratic Nonlinear Optical Properties. The second harmonic generation (SHG) powder tests were performed at 1.06 and at 1.34 μm according to the Kurtz and Perry method,¹³ on a series of 33 zwitterionic derivatives of type 2 recrystallized in aqueous ethanol, by comparison with the visible second harmonic signals of crystalline powdered samples of urea, POM (4-nitro-3-

(6) Meredith, G. In *Nonlinear Optical Properties of Organic and Polymeric Materials*; Williams, D. J., Ed.; 1983; ACS Symposium Series 233, 27.

(7) Marder, S. R.; Perry, J. W.; Schaefer, W. P. *Science* 1989, 245, 626.

(8) Marder, S. R.; Perry, J. W.; Schaefer, W. P. *J. Mater. Chem.* 1992, 2, 985.

(9) Okada, J. L.; Masaki, A.; Matsuda, H.; Nakanishi, H.; Kato, M.; Muramatsu, R.; Otsuka, M. *Jpn. J. Appl. Phys.* 1990, 29, 1112.

(10) Hassner, A.; Birnbaum, D.; Loew, L. M. *J. Org. Chem.* 1984, 49, 2546.

(11) Heck, R. F. *Palladium-Catalyzed Vinylation of Organic Halides; In Organic Reactions*; John Wiley & Sons Inc.: New York, 1982; Vol. 27, pp 345–389.

(12) Le Berre, A.; Etienne, A.; Dumaitre, B. *Bull. Soc. Chim. Fr.* 1970, 3, 946, 954.

(13) Kurtz, S. K.; Perry, T. T. *J. Appl. Phys.* 1966, 39, 3798.

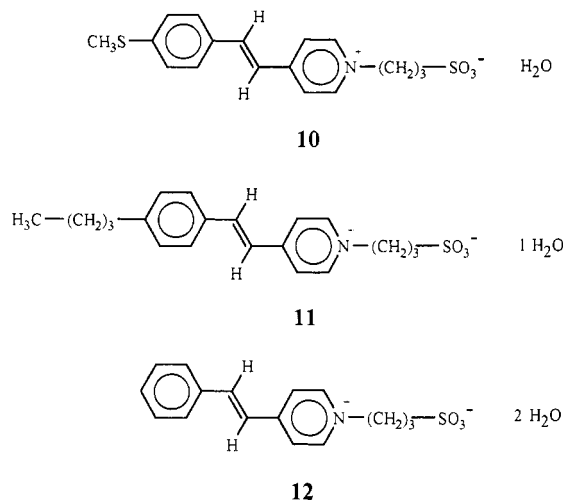


Figure 4. Molecular structure of MTSPS [4-(methylthio)-4'-(3-sulfonatopropyl)stilbazolium] (10), BSPS [4-*n*-butyl-4'-(3-sulfonatopropyl)stilbazolium] (11) and SPS [4-(3-sulfonatopropyl)stilbazolium] (12).

methylpyridine 1-oxide)¹⁴ and NPP (*N*-4-(nitrophenyl)-*L*-prolinol)¹⁵ used as references. From this first screening we found two new highly SHG efficient compounds relative to their transparency. The first is 4-(methylthio)-4'-(3-sulfonatopropyl)stilbazolium (10) further called MTSPS and the second is 4-*n*-butyl-4'-(3-sulfonatopropyl)stilbazolium (11) further called BSPS (Figure 4). The magnitude of the SHG powder test of MTSPS has been measured to be 370 times urea or 2.4 times NPP at 1.06 μm and for BSPS 10 times urea at 1.06 μm . These results underline the difficulty to obtain simultaneously a noncentrosymmetric packing together with an adequate arrangement of the molecules in the lattice. It is to be noticed that intense two-photon luminescence signals have often been observed on SHG-inactive materials, especially from compounds bearing a donor amino group. Such zwitterionic dyes bearing a donor amino group have been shown to be highly fluorescent previously, which made them of interest as electrochromic probes for membrane potential.¹⁰ It has also been shown that SHG could be detected from living cells stained with these dyes, which appears as the first study of their quadratic nonlinear optical properties.¹⁶

MTSPS crystals recrystallized from aqueous ethanol appear macroscopically as yellow needles. This first crystal modification is called MTSPS phase I. The elemental analysis of the tested powder attests the presence of one molecule of water per zwitterionic molecule. As for BSPS, it appears as a highly hygroscopic straw colored powder, making its interest for the elaboration of bulk crystals relatively less interesting.

Polymorphism Study. It is well-known that crystalline compounds often exhibit polymorphism that can afford drastic modifications of their SHG powder test signals. For example, it has been reported that 4-methoxy-4'-nitrotolane (MONT)¹⁷ presents three crystalline phases depending on the solvent of crystallization as well as

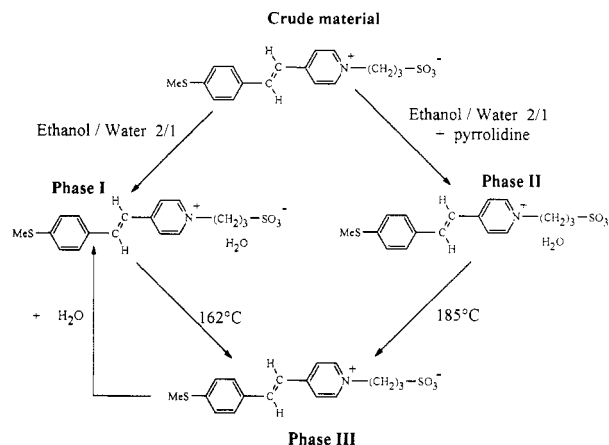


Figure 5. Various solid phases of MTSPS material and their mutual transformations.

4-methoxy-4'-nitro-2-cyanostilbene (CMONS),¹⁸ Since our molecules are heterocyclic analogs of stilbenes, we decided to check if such a polymorphism would occur. A wide screening over several crystallization conditions allowed us to find a new highly SHG active crystalline phase for MTSPS, which was obtained from crystallization in a 2/1 ethanol-water mixture containing 1 equiv of pyrrolidine relative to the amount of material in solution. This second crystal modification (called MTSPS-phase II) appears macroscopically as yellow-orange plates. The magnitude of its SHG powder test signal at 1.06 μm is 1.3 \times NPP (that means nearly 200 \times urea). Its elemental analysis indicates one molecule of water per zwitterionic molecule, like for phase I. The DSC diagram of this material indicates a transformation at 185 $^{\circ}\text{C}$ leading to a third phase (called MTSPS-phase III), which appears macroscopically as an orange powder and corresponds to a dehydrated product as shown by the elemental analysis. The same behavior has been observed for MTSPS-phase I which is transformed at 162 $^{\circ}\text{C}$ leading to the same dehydrated material. The Debye-Scherrer diffraction patterns of both phases obtained by heating phase I and phase II of MTSPS are identical. This anhydrous MTSPS-phase III material is SHG inactive. Recrystallization of phase III powder from water afforded again phase I crystals. The general behavior of MTSPS material, checked by DSC analyses, showing the transformations between its different phases is summarized in Figure 5.

Some of the SHG inactive crystalline materials from our first screening were also submitted to crystallization in the presence of pyrrolidine, to check the possible formation of a new crystalline phase. We met success with (3-sulfonatopropyl)stilbazolium (12, further called SPS in the text, Figure 4). Thus, recrystallization of 12 from a 2/1 ethanol-water mixture afforded SPS-phase I material as straw-colored needles which were SHG inactive. The elemental analysis of these crystals attests the presence of one molecule of water for each molecule of stilbazolium, while recrystallization from a 2/1 ethanol-water mixture containing 1 equiv of pyrrolidine afforded a new crystalline phase of SPS (called SPS-phase II) that appears macroscopically as nearly white plates. In this later case the elemental analysis indicates the presence of two molecules of water for each stilbazolium entity. The magnitude of SPS-phase II SHG powder test at 1.06 μm has been measured to be 15 \times urea. Heating SPS-phase I at 86 $^{\circ}\text{C}$ and SPS-phase II at 116 $^{\circ}\text{C}$ leads to the same dehydrated crystalline material, called SPS-phase III, that

(14) Zyss, J.; Chemla, D. S.; Nicoud, J. F. *J. Chem. Phys.* 1981, 74, 4800.

(15) Zyss, J.; Nicoud, J. F.; Coquillay, M. *J. Chem. Phys.* 1984, 81, 4160.

(16) Huang, J. Y.; Lewis, A.; Loew, L. *Biophys. J.* 1988, 53, 665.

(17) Tabei, H.; Kurihara, T.; Kaino, T. *Appl. Phys. Lett.* 1987, 50, 680.

(18) Oliver, S. N.; Pantelis, P.; Dunn, P. L. *Appl. Phys. Lett.* 1990, 56, 307.

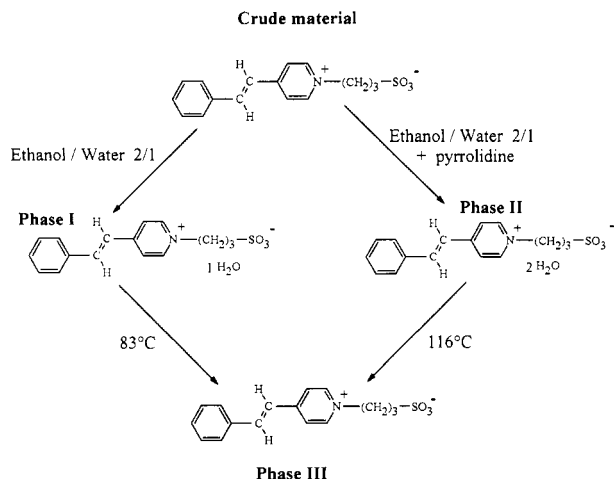


Figure 6. Various solid phases of SPS material and their mutual transformations.

Compound 2	λ (SHG)	$n = 2$	$n = 3$	$n = 4$
D = CH ₃ S	1.06 μm	++	10, MTSPS ++++ phase I: 2.4xNPP phase II: 1.3xNPP phase III: inactive	-
	1.34 μm	++	++++	-
D = nC ₄ H ₉	1.06 μm	/	11, BSPS ++	/
	1.34 μm	/	/	/
D = H	1.06 μm	-	12, SPS ++ phase I: inactive phase II: 15 x urea phase III: inactive	-
	1.34 μm	-	++	-

Figure 7. SHG powder test activity at 1.06 μm and 1.34 μm of zwitterionic stilbazolium materials 10, 11, and 12 (Figure 4), as a function of the alkyl chain length between the ionic parts. Given the broad range of sizes of crystalline particles, the preliminary powder tests were not quantified. + denotes a signal comparable to or a few times greater than that of urea, ++, +++, and ++++ refer to 1, 2, or 3 orders of magnitude greater signals respectively. - denotes no eye detectable SHG signal.

is SHG inactive. The behavior of SPS material, checked by DSC analyses, showing the different phases is summarized in Figure 6. The effect of the alkyl chain length between the ionic parts of the zwitterion can be seen in Figure 7 for the three selected compounds 10, 11, and 12. The MTSPS analog with $n = 2$ is the only SHG active one in the series 2, $n = 2$ (4 compounds tested). We observed that none of the 11 zwitterionic 4-sulfonatobutyl-*N*-stilbazolium compounds ($n = 4$) that we studied show a positive SHG powder test. From the 33 derivatives tested in total, only 6 compounds were SHG active. From our powder tests results one can conclude only that the (3-sulfonatopropyl)pyridinium entity appears to lead to a higher propensity of giving noncentrosymmetric crystal packing.

X-ray Crystal Structures Analyses. Crystal structure investigations were undertaken to study the orientation of the chromophores in the lattice, the role played by the water molecule, possible intermolecular interactions in the solid state, and the actual conformation of the molecules in comparison with that calculated by molecular

Table 1. X-ray Experimental Details for MTSPS-H₂O-Phase I Crystal Structure Determination

formula	C ₁₇ H ₁₉ NO ₃ S ₂ ·H ₂ O
mol wt	367.48
color	yellow
crystal system	monoclinic
a (Å)	10.380(3)
b (Å)	11.124(3)
c (Å)	6.968(2)
β (deg)	99.93(2)
vol (Å ³)	863.8
Z	2
D_{calc} (g·cm ⁻³)	1.413
wavelength (Å)	1.5418
μ (cm ⁻¹)	29.259
space group	$P2_1$
diffractometer	Philips PW1100/16
crystal dimension (mm)	0.22 × 0.28 × 0.32
temp (°C)	-100
radiation	Cu K α graphite monochromated
mode	$\theta/2\theta$ flying step-scan
scan speed (deg ⁻¹)	0.020
step width (deg)	0.05
scan width (deg)	0.90 + 0.14 tan(θ)
octants	$\pm h + h + l$
θ min/max (deg)	3/56
no. of data collected	1290
no. of data with $I > 3\sigma(I)$	1115
abs min/max	0.83/1.14
$R(F)$	0.039
$Rw(F)$	0.066
p	0.08
GOF	1.647

modeling. Single crystals of the two SHG-active crystalline phases of MTSPS suitable for X-ray diffraction studies were grown by slow evaporation of suitable solutions. However we were unable to get good-quality crystals of the SHG-active SPS-phase II for X-ray structural investigations.

X-ray Crystal Structure Determination of 4-(Methylthio)-4'-(3-sulfonatopropyl)stilbazolium (10, MTSPS-Phase I). The crystal structure of 4-(methylthio)-4'-(3-sulfonatopropyl)stilbazolium monohydrate-phase I C₁₇H₁₉NO₃S₂·H₂O (10, MTSPS-phase I) was determined. Single crystals of MTSPS-phase I suitable for X-ray diffraction were grown by slow evaporation of a 2/1 ethanol-water solution of the compound. A single crystal of 0.22 mm × 0.28 mm × 0.32 mm was selected. It crystallizes in the noncentrosymmetric monoclinic, space group $P2_1$. Table 1 shows the final unit-cell dimensions and experimental details. Atomic coordinates, selected bond lengths and bond angles are supplied in Tables 2–4. There are two zwitterionic moieties and two water molecules in the unit cell, confirming the ratio of one water molecule per zwitterionic entity deduced from the elemental analysis; Figure 8 displays one zwitterionic moiety together with the labeling scheme used. The atoms S1 to C15 of the central part of the zwitterionic moiety are nearly coplanar (maximum deviation C9: 0.084(6) Å), therefore, the conformation of the (methylthio)stilbazolium part of MTSPS backbone is favorable to an efficient intramolecular charge transfer between the methylthio donor group and the pyridinium acceptor. The 3-sulfonatopropyl component is interesting because it does not create a ring with the nitrogen of the pyridinium, but on the contrary it is opened and makes an angle of 37.6° with the mean plane of the stilbazolium moiety (Figure 8). The shortest distance between the pyridinium nitrogen and the nearest oxygen atom of the sulfonato group is equal to 5.5 Å (N...O2). We also found a similar conformation for an isolated MTSPS molecule in the gas phase, by molecular

Table 2. Table of Positional Parameters for MTSPS-H₂O-Phase I Crystal and Their Esd's^a

atom	x	y	z	B (Å ²)
S1	0.2384(1)	0.256	0.4647(2)	2.57(3)
S2	1.1173(1)	0.7289(1)	-0.9422(2)	2.20(3)
O1	1.1680(4)	0.7543(4)	-1.1184(5)	2.88(8)
O2	1.0608(4)	0.8249(4)	-0.8626(7)	3.35(9)
O3	1.2124(4)	0.6721(4)	-0.7985(7)	3.9(1)
N	0.7126(4)	0.5156(3)	-0.7752(6)	1.74(9)
C1	0.1036(5)	0.3506(6)	0.4457(9)	3.2(1)
C2	0.3157(5)	0.2965(5)	0.2695(8)	1.9(1)
C3	0.4379(5)	0.2547(5)	0.2634(7)	2.0(1)
C4	0.5055(5)	0.2807(5)	0.1153(8)	2.3(1)
C5	0.4481(5)	0.3507(5)	-0.0365(8)	2.0(1)
C6	0.3233(5)	0.3946(5)	-0.0291(8)	2.3(1)
C7	0.2575(5)	0.3668(5)	0.1147(8)	2.4(1)
C8	0.5243(5)	0.3779(5)	-0.1903(8)	2.0(1)
C9	0.4909(5)	0.4507(5)	-0.3326(8)	2.2(1)
C10	0.5696(5)	0.4718(4)	-0.4812(7)	1.7(1)
C11	0.5201(5)	0.5386(5)	-0.6439(8)	2.1(1)
C12	0.5909(5)	0.5585(5)	-0.7869(8)	1.9(1)
C13	0.7640(5)	0.4513(5)	-0.6204(8)	2.2(1)
C14	0.6962(6)	0.4296(5)	-0.4801(8)	2.4(1)
C15	0.7937(5)	0.5384(5)	-0.9284(8)	2.2(1)
C16	0.9052(5)	0.6163(5)	-0.8585(8)	2.2(1)
C17	0.9856(6)	0.6344(5)	-1.0170(9)	2.4(1)
Ow	0.7724(6)	0.1108(5)	0.4109(7)	5.4(1)

^a Anisotropically refined atoms are given in the form of the isotropic equivalent displacement parameter defined as $\frac{1}{3}[a^2\beta(1,1) + b^2\beta(2,2) + c^2\beta(3,3) + ab(\cos \gamma)\beta(1,2) + ac(\cos \beta)\beta(1,3) + bc(\cos \alpha)\beta(2,3)]$.

Table 3. Table of Bond Distances (Å) for MTSPS Molecule 10 (from Phase I Crystals)^a

atom 1	atom 2	distance	atom 1	atom 2	distance
S1	C1	1.794(7)	C4	C5	1.406(9)
S1	C2	1.763(6)	C5	C6	1.409(9)
S2	O1	1.449(4)	C5	C8	1.475(9)
S2	O2	1.456(5)	C6	C7	1.349(9)
S2	O3	1.452(5)	C8	C9	1.33(1)
S2	C17	1.791(7)	C9	C10	1.449(8)
N	C12	1.355(9)	C10	C11	1.416(9)
N	C13	1.363(8)	C10	C14	1.408(9)
N	C15	1.495(8)	C11	C12	1.358(9)
C2	C3	1.373(8)	C13	C14	1.326(9)
C2	C7	1.425(9)	C15	C16	1.51(1)
C3	C4	1.381(8)	C16	C17	1.511(9)

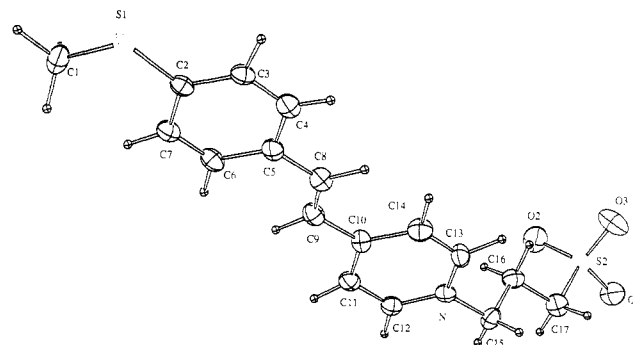
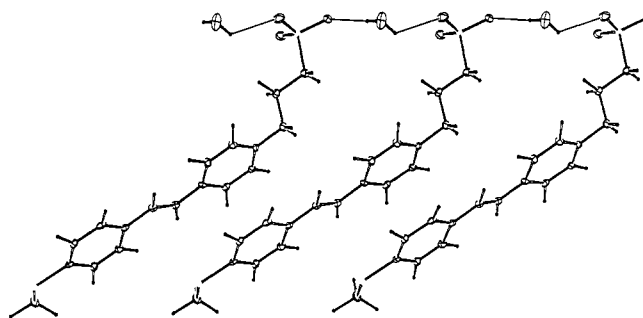
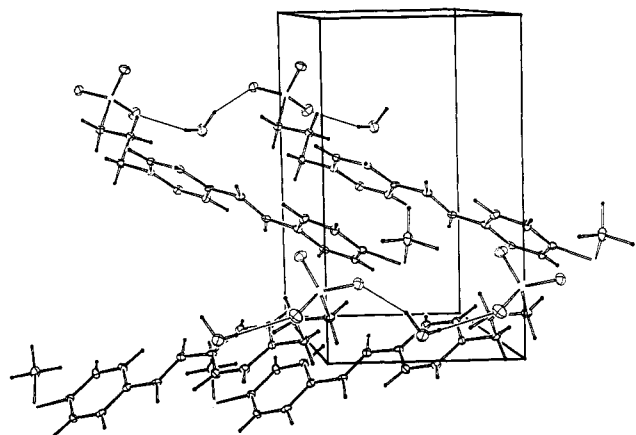
^a Numbers in parentheses are estimated standard deviations in the least significant digits.

Table 4. Table of Bond Angles (deg) for MTSPS Molecule 10 (from Phase I Crystals)^a

atom 1	atom 2	atom 3	angle	atom 1	atom 2	atom 3	angle
C1	S1	C2	102.7(3)	C4	C5	C8	118.1(5)
O1	S2	O2	112.5(3)	C6	C5	C8	123.6(6)
O1	S2	O3	112.5(3)	C5	C6	C7	121.3(6)
O1	S2	C17	105.1(3)	C2	C7	C6	120.6(5)
O2	S2	O3	112.7(3)	C5	C8	C9	126.0(6)
O2	S2	C17	106.5(3)	C8	C9	C10	122.9(6)
O3	S2	C17	106.9(3)	C9	C10	C11	120.1(5)
C12	N	C13	120.1(5)	C9	C10	C14	125.0(6)
C12	N	C15	121.4(5)	C11	C10	C14	114.9(5)
C13	N	C15	118.6(5)	C10	C11	C12	121.4(6)
S1	C2	C3	117.8(5)	N	C12	C11	120.3(5)
S1	C2	C7	124.0(4)	N	C13	C14	120.8(5)
C3	C2	C7	118.1(6)	C10	C14	C13	122.5(6)
C2	C3	C4	122.0(5)	N	C15	C16	112.4(5)
C3	C4	C5	119.8(5)	C15	C16	C17	110.2(5)
C4	C5	C6	118.2(6)	S2	C17	C16	111.8(5)

^a Numbers in parentheses are estimated standard deviations in the least significant digits.

modeling using the SIBYL software (Tripos Associates) with the Tripos's force field 5.1. The ribbon like molecules are linked together from cell to cell along the *c* axis by water molecules, giving strong hydrogen bonds between

**Figure 8.** ORTEP plot of MTSPS molecule (10), showing the numbering scheme used. Ellipsoids are scaled to enclose 50% of the electronic density. Hydrogen atoms have arbitrary radii.**Figure 9.** Hydrogen bond network displayed by the water molecule linking two neighboring sulfonate anions, along the *c* axis.**Figure 10.** View of the unit cell of MTSPS-H₂O-phase I crystal showing the H-bonds network, the head to tail stacking along the 2₁ screw axis and the donor/acceptor π interactions between sheets.

H₂O and O3 (Ow...O3 = 2.779 Å, H2O...O3 = 2.23 Å) and between H21 and O1 (Ow...O1 = 2.828 Å, H21...O1 = 1.92 Å) forming sheets of parallel ribbons as shown in Figure 9. Within a sheet, the ribbons are arranged so that the donor part of one ribbon faces the acceptor part of the translated ribbon. The distance between the centroids of the (N1C10-C13) and (C2-C7) rings is equal to 3.612 Å giving rise to π interactions in the sheets. In the crystal, pairs of sheets are related by the 2₁ screw axis of the space group giving a head to tail packing as shown in Figure 10. The shortest contact interaction between sheets are listed in Table 5. The water molecule also gives weak intersheets contacts (>3.6 Å). For P2₁ space group, it has been demonstrated from the oriented gas model that the macroscopic NLO susceptibility $\chi^{(2)}_{YXX}$ is correlated to $f(\theta) = \cos \theta \sin^2 \theta$, where θ is the angle between the charge-

Table 5. Intermolecular Contacts Less than 3.6 Å in MTSPS-Phase I Crystals

		translation ^a		
		tx	ty	tz
S1--C12	3.544	1	-1	0
O1--C13	3.156	2	0	-2
O1--C4	3.401	2	0	-1
O1--C15	3.476	2	0	-2
O1--C1	3.506	1	0	-1
O1--N	3.528	2	0	-2
O2--C14	3.406	2	0	-1
O2--C15	3.501	2	0	-2
C4--C12	3.565	1	1	-1

^a Equivalent fractional coordinates generated from independents x, y, z by $x' = -x + tx, y' = 1/2 + y + ty, z' = -z + tz$.

Table 6. Crystallographic Details for MTSPS-H₂O-Phase II Crystals (from Ref 20)

formula	C ₁₇ H ₁₉ NO ₃ S ₂ H ₂ O
formula wt	367.47
crystal system	orthorhombic
space group	Pc2 ₁ b
Z	4
a (Å)	6.989
b (Å)	12.430
c (Å)	20.59
D _x	1.365 g cm ⁻³
crystal dimensions (mm)	0.64 × 0.35 × 0.22

transfer axis and the b axis of the crystal.¹⁹ If we assume that the charge-transfer axis of MTSPS lies between S1 and N, then the θ value is equal to 73.5°. The observed orientation of the stilbazolium backbone is then not optimal since the maximum of the function $f(\theta) = \cos \theta \sin^2 \theta$ is obtained for $\theta = 54.7^\circ$ [$f(\theta)_{\max} = 0.385$]. Here $f(\theta) = 0.261$; hence one may assume that a 4-(alkylthio)-4'-(3-sulfonatopropyl)stilbazolium derivative having an optimized packing would be 3.5 times more efficient than NPP for the same transparency range.¹⁵ This result shows that the additional dipole moment strategy is a valuable crystal engineering strategy for $\chi^{(2)}$ crystalline NLO materials.

X-ray Crystal Structure of 4-(Methylthio)-4'-(3-sulfonatopropyl)stilbazolium (10, MTSPS-Phase II). The crystal structure of MTSPS-phase II has been also resolved, the results being reported in a separate paper.²⁰ We recall here the fundamental results for comparison. The compound crystallizes in the orthorhombic, noncentrosymmetric space group Pc2₁b. The general outlines of the structure are given in Table 6. Here we must notice again the role played by the water molecule which is the center of five hydrogen bonds. The shortest H-bonds occur between the H atoms of the water molecule and two oxygen atoms of two different sulfonate groups SO₃⁻. Hence the water molecules induce a cohesive tridimensional network between the MTSPS molecules, a key role for the molecular packing cohesion. Along the a axis, the molecules are translationally stacked, the interplanar distance between stilbazolium planes being short and equal to 3.20 Å. This could mean again that an intermolecular overlapping of the (methylthio)phenyl ring of one molecule and the pyridinium of another one is possible, leading to an intermolecular charge transfer.

Molecular Properties of Zwitterionic Stilbazolium Compounds. To fully characterize the three new materi-

als 10–12, the hyperpolarizability β measurements were performed by the classical electric-field-induced second harmonic generation (EFISH) technique, using a Q-switched, mode-locked Nd³⁺:YAG laser, emitting at 1.34 μm in order to avoid undesirable absorption of the second harmonic. The only values reported so far for β values of a stilbazolium chromophore came from Lupo *et al.*, who first determined $\chi^{(2)}$ values of a Langmuir–Blodgett monolayer from second harmonic generation at 1.06 μm and then deduced the molecular β values by using the oriented gas model.²¹ For example, β value of derivative 1 bearing a methoxy donor group (1: D = OMe, X⁻ = counteranion) is reported to be 150×10^{-30} esu. No EFISH results have been reported so far in the literature since stilbazolium salts are ionic species that cannot be oriented under an electric field in solution. Our zwitterionic compounds containing the stilbazolium NLO chromophore are neutral species, their solutions are not electrically conductive so that the EFISH measurements can be performed. However since their solubility in classical EFISH nonaqueous solvents are too low, we decided to synthesize soluble analogs bearing bulky substituents or long alkyl chains to improve the solubility. Hence, we prepared 4-(decylthio)-4'-(3-sulfonatopropyl)stilbazolium (13) and 3,5-di-*tert*-butyl-4-(3-sulfonatopropyl)stilbazolium (14) respectively as soluble analogous derivatives of MTSPS and SPS. For the synthesis of 13, the precursory 4-(n -decylthio)benzaldehyde was obtained by an aromatic nucleophilic substitution (S_NAr) with n -decylthiolate anion on 4-fluorobenzaldehyde according to Cogolli and Chinelli's procedures.^{22,23} As for synthesis of 14, the 3,5-di-*tert*-butylbenzaldehyde starting aromatic aldehyde was obtained by Newman and Lee's method.²⁴ The EFISH measurements were realized in chloroform solutions. Since the scalar product $\mu_0\beta$ is finally derived from these measurements, the experimental values of the ground-state dipole moments μ_0 were measured in chloroform according to the classical method proposed originally by Hedestrand and completed more recently by Moll and Lippert.^{25,26} The results are summarized in Table 7.

To get a good appreciation of the interest of a new class of molecules for nonlinear optics, the EFISHG measurement of the chromophore must always be completed with a description of its transparency range, in order to evaluate its nonlinearity/transparency tradeoff.

The UV-visible spectra of 2 shows a strong broad absorption which can be attributed to the intramolecular charge transfer (ICT) between the donor group and the acceptor pyridinium ring. Due to the width and the intensity of this absorption band, the oscillator strength associated with this ICT transition must be important and according to the two-level model, a large molecular hyperpolarizability β could be anticipated. For the thioalkyl donor group the absorption maximum of a 4-substituted 4'-(n -sulfonatoalkyl)stilbazolium derivative lies in the same range as the corresponding 4-substituted 4'-nitrostilbene (Table 8). The λ_{\max} of the ICT transition appears to be much more dependent on the nature of the

(21) Lupo, D.; Prass, W.; Scheunemann, U.; Laschewsky, A.; Ringsdorf, H.; Ledoux, I. *J. Opt. Soc. Am. B* 1988, 5, 2.

(22) Cogolli, P.; Maiolo, F.; Testaferri, L.; Tingoli, M.; Tiecco, M. *J. Org. Chem.* 1979, 44, 2641.

(23) Chinelli, D.; Testaferri, L.; Tiecco, M.; Tingoli, M. *Synthesis* 1982, 475.

(24) Newman, M. S.; Lee, L. F. *J. Org. Chem.* 1972, 37, 4468.

(25) Hedestrand, G. *Z. Phys. Chem.* 1924, B 2, 423.

(26) Moll, F.; Lippert, E. *Z. Elektrochem.* 1954, 58, 553.

(19) Zyss, J.; Oudar, J. L. *Phys. Rev. A* 1982, 26, 2028.

(20) Gautier-Luneau, I.; Serbutoviez, C.; Nicoud, J. F. *Z. Kristallogr.* 1994, 209, 531.

Table 7. CT Absorption Peak (λ_{\max}), Molecular Dipole Moment (μ_0), Hyperpolarizability β (at 1.34 μm), and $\beta(0)$ (Static) of MTSPS and SPS Analogs

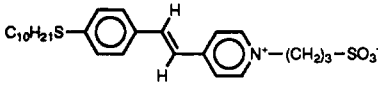
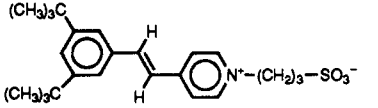
compound	λ (CT) (nm)	dipole moment μ (D)	β (1.34 μm) (10^{-30} esu)	$\beta(0)$ (static) (10^{-30} esu)
 13 soluble analog of MTSPS	390	16	61	37
 14 soluble analog of SPS	366	10	15.9	10

Table 8. Comparison of the CT Absorption Maximum between Stilbazolium and 4-Nitrostilbene Chromophores Substituted by the Same Donor Group

donor group	CT λ_{\max} (nm) 4-substituted 4'-[n-sulfonatoalkyl]-stilbazolium (2)	CT λ_{\max} (nm) 4-substituted 4'-nitrostilbene
N(CH ₃) ₂	n = 4, 477	436
SMe	n = 3, 398	382
CH ₃	n = 3, 363	371

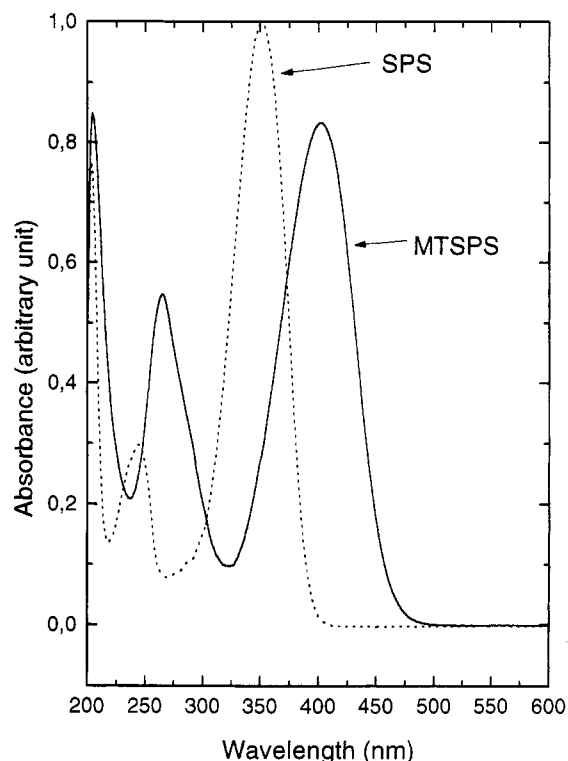
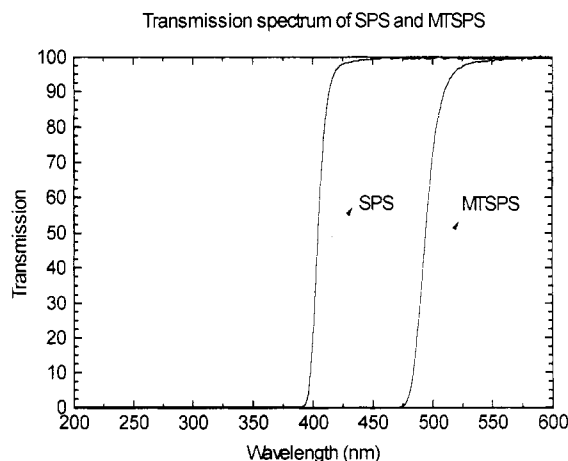
donor group in the stilbazolium series than in the one of the nitrostilbene derivatives. But when opposed to a weak donor group (or none as in SPS), we can expect some improvement for the nonlinearity/transparency tradeoff.

The UV-visible absorption spectra of a 2.7×10^{-5} M MTSPS solution and 5×10^{-5} M SPS solution in absolute ethanol are shown in Figure 11. MTSPS exhibits a strong charge-transfer transition centered at $\lambda_{\max} = 398$ nm responsible for the yellow coloration of the compound with an extinction coefficient $\epsilon_{\max} = 30\,000 \text{ M}^{-1} \text{ cm}^{-1}$. Regarding SPS, it presents an absorption maximum $\lambda_{\max} = 350$ nm and an extinction coefficient $\epsilon_{\max} = 20\,000 \text{ M}^{-1} \text{ cm}^{-1}$. The transmission cutoff obtained from a spectrum of a saturated solution in ethanol are respectively at $\lambda = 490$ nm for MTSPS and $\lambda = 405$ nm for SPS (Figure 12). These absorption data allowed us to calculate the corresponding static $\beta(0)$ values by modeling the dispersion of β for a two-level system according to the eq 1,^{27,28} where W is the

$$\beta(\omega) = \beta(0) \frac{W^4}{[W^2 - (\hbar\omega)^2][W^2 - (2\hbar\omega)^2]} \quad (1)$$

energy of the charge-transfer transition, ω the frequency of the laser light and \hbar the Planck constant/ 2π . According to this equation, $\beta(0)$ is equal to 37×10^{-30} esu for MTSPS and 10×10^{-30} esu for SPS. When opposed to strong donor groups, the pyridinium-withdrawing power is equivalent to the one of the nitrophenyl group, for an equivalent range of transparency. For example, the static hyperpolarizability β_0 of MTSPS has the same magnitude as that of 4-(methylthio)-4'-nitrostilbene, the latter being equal to 43×10^{-30} esu.²⁹ Such results were expected since the value of the Hammett coefficient of the pyridinium lies in the same range as the nitrophenyl one.

The large ground-state dipole moments of these molecules are the sum of two contributions, one from the donor-acceptor charge transfer (μ_{ct}) and the other from

**Figure 11.** UV-visible absorption spectra of MTSPS and SPS solutions in ethanol.**Figure 12.** Transmission cutoff of MTSPS and SPS saturated solutions in ethanol.

the zwitterionic (3-sulfonatopropyl)-1-pyridinium part ($\mu_{\text{zwitterion}}$). If we assume that μ_{ct} for a 4-substituted stilbazolium chromophore is close to the one of a 4-nitrostilbene analog, we notice that the contribution of the zwitterionic moiety is very effective. This result can be correlated to

(27) Oudar, J. L. *J. Chem. Phys.* 1977, 67, 446.(28) Barzoukas, M.; Fremaux, P.; Josse, D.; Kajzar, F.; Zyss, J. *Mater. Res. Soc. Proc.* 1988, 109, 3774.(29) Barzoukas, M.; Fort, A.; Klein, G.; Boeglin, A.; Serbutoviez, C.; Oswald, L.; Nicoud, J. F. *J. Chem. Phys.* 1992, 164, 395.

the sulfonatoalkyl chain conformation. On one hand, when a (3-sulfonatopropyl)stilbazolium entity is substituted in position 4 by a strong donor group, such as methylthio, the positive charge on the pyridinium nitrogen is lowered by the charge transfer, the anionic sulfonato group is less attracted by the pyridinium, hence the aliphatic ion bridge can adopt the well-known all-trans conformation that creates a large dipole moment outside of the charge-transfer axis. On the other hand, when no donor group or only weak donor groups are present the positive charge on the pyridinium is not very delocalized and can attract the sulfonato group leading to a weaker additional dipole moment. This could be the origin of the lower dipole moment (10 D) measured for the SPS analog, in comparison with the MTSPS analog (16 D, Table 7). The partition of the ground-state dipole moment between the contributions of the charge-transfer system and the zwitterionic moiety could appear somewhat speculative since the dipole moment of the simple zwitterionic (3-sulfonatopropyl)-1-pyridinium molecule is not known, but our analysis is supported by the conformation of MTSPS molecule in the crystal phases and that obtained by molecular modeling using the SYBYL software (Tripos Associates, Inc.).

Estimation of Quadratic Nonlinear Susceptibilities Using the Oriented Gas Model. In most organic molecular crystals, the energy of van der Waals or hydrogen bonds responsible for the intermolecular cohesion is much weaker, by 1 or 2 orders of magnitude, than that of intramolecular chemical bonds. Molecules remain therefore distinguishable entities and the macroscopic nonlinear response of the materials may be described using a simple summation scheme, following the oriented gas model, whereby the crystalline susceptibility d_{IJK} originates essentially from the β_{ijk} mediated anharmonic response of molecular oscillators, given by eq 2.¹⁹

$$d_{IJK}(-2\omega; \omega, \omega) = N f_I^{2\omega} f_J^{\omega} f_K^{\omega} \sum_{s=1}^n \cos(I, i(s)) \cos(J, j(s)) \cos(K, k(s)) \beta_{ijk}(s) \quad (2)$$

The summation is performed over all n molecules (indexed by s) in the unit cell, the cosine product terms representing the rotation from the molecular reference frame (i, j, k) onto the crystal frame (I, J, K). N is the number of unit cells per unit volume, and the Lorentz local-field factors f , given by $f_I^{2\omega} = [(n_I^{\omega, 2\omega})^2 + 2]/3$, account for mutual polarization effects between neighboring molecules. One may here rely on this simple molecules oriented gas model, rather than to invoke possible excitonic phenomena, in the case of off-resonant excitations such as considered now. In the transparency range of the material, no significant intermolecular interactions as related to excitonic considerations have to be taken into account. d_{IJK} can be expressed in a more concise form as in eq 3,¹⁹ where b_{IJK} is the crystalline nonlinearity per

$$d_{IJK} = N f_I^{2\omega} f_J^{\omega} f_K^{\omega} b_{IJK} \quad (3)$$

molecule which, for a given β value, depends on the symmetry of the crystalline point group only. In the following, we will consider a purely one-dimensional β tensor, a relevant approximation in the case of the highly

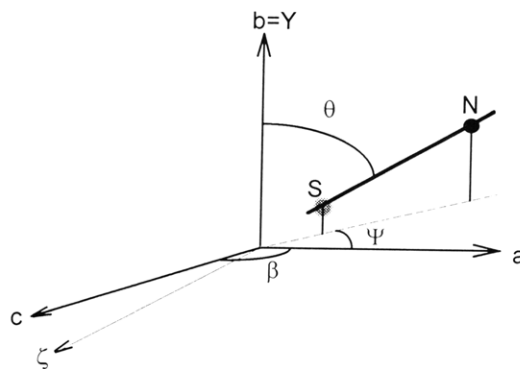


Figure 13. Schematic view of the orientation of the intramolecular charge transfer axis S_1-N in the macroscopic reference frame (a, b, ζ).

anisotropic MTSPS molecule. In ref 19, b_{IJK} expressions are given for all noncentrosymmetric point groups.

The validity of this oriented-gas model has already been assessed on well-documented crystals such as NPP^{15,30} or NPAN.³¹ For NPP at 1.34 μm , $\beta = 20 \times 10^{-30}$ esu,⁴ and the value of the phase-matched refractive index is $n^\omega = n^{2\omega} = 1.85$,³⁰ leading to a local field factor $f = 5.9$. Using the oriented gas model, a simple calculation leads, for NPP, to $d_{YXX} = 69$ pm/V and $d_{YYY} = 25$ pm/V at 1.34 μm ; these values are reasonably close to those found by direct experimental SHG measurements, at the same wavelength, on single crystalline samples,³⁰ i.e., $d_{YXX} = 60$ pm/V and $d_{YYY} = 20$ pm/V.

As NPP belongs to the same $P2_1$ space group (point group 2) as MTSPS-phase I, and the NPP molecule exhibits similar anisotropic features, the same model can be reliably applied to estimate the crystalline nonlinearity of MTSPS (phases I and II), taking similar refractive index values as that of NPP, the maximum absorption wavelengths λ_{max} being identical.⁴ According to the notations of ref 19, a simplified description of the crystalline structure of MTSPS-phase I is given in Figure 13. Assuming a one-dimensional intramolecular charge transfer, the vector part of the hyperpolarizability tensor is aligned, in a first approximation, along the S_1-N axis. θ and ψ are the angular parameters defining the molecular orientation relatively to a macroscopic reference frame (a, b, ζ), where b is the 2-fold symmetry axis, identical to the dielectric Y axis, (a, ζ) is one plane. From the atomic coordinates of the S_1 and N atoms we infer $\theta = 73.5^\circ$ and $\psi = -53^\circ$. The orientation of the molecular plane with respect to the macroscopic reference frame can be also deduced from crystallographic data: this plane is tilted by 54.4° with the b axis, and its intersection with the (a, ζ) plane makes an angle of -28.64° with respect to a .

It must be pointed out that this structure is close to that of MTSPS-phase II:²⁰ the θ value is almost the same ($\theta = 73.3^\circ$ for MTSPS-phase II), and the value of the tilt angle between the molecular plane and the b axis is very similar (50.4°). Differences between MTSPS-phase I and MTSPS-phase II are minor: the volume per unit cell is twice larger in the case of the orthorhombic form (MTSPS-phase II) but, considering that the cell contains $Z = 4$ molecules instead of 2 for the $P2_1$ group, the mean molecular volume remains similar in both structures.

(30) Ledoux, I.; Lepers, C.; Périgaud, A.; Badan, J.; Zyss, J. *Opt. Commun.* **1990**, *80*, 149.

(31) Morita, R.; Vidakovic, P. *Appl. Phys. Lett.* **1992**, *61*, 2854.

Table 9. Estimated Values of the Second Harmonic d_{IJK} and Pockels Electrooptic r_{IJK} Coefficients for MTSPS-Phase I and MTSPS-Phase II Crystals

	MTSPS-phase I		MTSPS-phase II		
b_{IJK}	$b_{YXX} = \cos \theta \sin^2 \theta$	$b_{YYY} = \cos^3 \theta$	$b_{YYY} = \cos^3 \theta$	$b_{YXX} = \cos^2 \psi \cos \theta \sin^2 \theta$	$b_{YZZ} = \sin^2 \psi \cos \theta \sin^2 \theta$
angular parameters	$\theta = 73.5^\circ$	$\psi = -53^\circ$	$\theta = 73.3^\circ$	$\psi = -27.4^\circ$	
d_{IJK}	d_{YXX}	d_{YYY}	d_{YYY}	d_{YXX}	d_{YZZ}
$\lambda = 1.34 \mu\text{m}$	100 pm/V	8.9 pm/V	8 pm/V	70 pm/V	19 pm/V
$\lambda = 0$ (static)	60 pm/V	5.2 pm/V	4.8 pm/V	42 pm/V	11 pm/V
r_{IJK}^ω ($\lambda = 1.34 \mu\text{m}$)	-26 pm/V	-2.3 pm/V	-2.0 pm/V	-18 pm/V	-4.8 pm/V
r_{IJK} (static)	-24 pm/V	-2.2 pm/V	-1.9 pm/V	-17 pm/V	-4.6 pm/V

The estimated values, for both MTSPS-phase I and MTSPS-phase II structures, of the second harmonic d_{IJK} and Pockels electrooptic r_{IJK} coefficients are given in Table 9, taking the same local field factors as that of NPP, in view of their similar linear optical properties. According to the data from ref 19, the ψ value is found to be equal to 27.4° for MTSPS-phase II. d_{IJK} values are given at $1.34 \mu\text{m}$, taking $\beta_{\text{MTSPS}} = 61 \times 10^{-30}$ esu according to EFISH measurements at $1.34 \mu\text{m}$. The corresponding "static" values at zero frequency are inferred from the previous ones using the classical two-level dispersion model.²⁷

We have also reported the electro-optic (EO) coefficients r_{IJK}^ω at $\lambda^\omega = 1.34 \mu\text{m}$, r_{IJK}^ω being inferred from d_{IJK}^ω according to relation 4,³² where d_{IJK}^ω is a simplified

$$r_{IJK}^\omega = -4d_{IJK}^\omega/n_\omega^4 \quad (4)$$

notation for $d_{IJK}(-\omega; \omega, 0)$, and n_ω the refractive index at $1.34 \mu\text{m}$. $d_{IJK}(-\omega; \omega, 0)$ and $d_{IJK}(-2\omega; \omega, \omega)$ are related by the dispersion model of eq 5 defined in ref 32, where

$$\frac{d_{IJK}(-\omega; \omega, 0)}{d_{IJK}(-2\omega; \omega, \omega)} = \frac{f_I^\omega f_J^\omega f_K^0 \beta(-\omega; \omega, 0)}{f_I^{2\omega} f_J^\omega f_J^\omega \beta(-2\omega; \omega, \omega)} \quad (5)$$

$f_{IJK}^{\omega, 2\omega}$ are Lorentz-Lorenz local field factors as defined previously, while $f_K^0 = \epsilon(0)(\epsilon_\infty + 2)/[\epsilon_\infty + 2\epsilon(0)]$ is the Onsager correction, and ϵ_∞ (respectively $\epsilon(0)$) is the dielectric constant at optical (respectively zero) frequency. Here we take $\epsilon_\infty = (n_{2\omega})^2$ and $\epsilon(0) = 3$, corresponding to a typical order of magnitude for dielectric constants of organic molecular crystals.³² $\beta(-\omega; \omega, 0)$ can be deduced from $\beta(-2\omega; \omega, \omega)$ using the two-level model, leading to eq 6.³² These values correspond to the $\omega = 0$ extrapolation

$$\frac{\beta(-\omega; \omega, 0)}{\beta(-2\omega; \omega, \omega)} = \frac{(3\omega_0^2 - \omega^2)(\omega_0^2 - 4\omega^2)}{3\omega_0^2(\omega_0^2 - \omega^2)} \quad (6)$$

of the electronic polarization contributions, regardless of possible non negligible vibrational contributions.³³ We have also reported the r_{IJK} values corresponding to the static EO coefficients, deduced from the static d_{IJK} values according to eq 4, using a "static" refractive index value $n(\text{static})$. It must be pointed out that local field factors and r_{IJK} values, deduced from experimental data using eqs 4 and 5, are significantly affected by the refractive index values at ω , 2ω , or zero frequency. We choose here, assuming similar n values as compared to NPP crystal, $n(\omega) = 1.78$ and $n(\text{static}) = 1.75$ in eq 4 to calculate r_{IJK}^ω and $r_{IJK}(\text{static})$, respectively. These values are only approximate, in the absence, at this stage, of large, high-quality crystals for refractive index measurements.

The phase-matching conditions of MTSPS-phases I and II crystals being unknown at this stage, it is difficult to give a precise estimate of the corresponding effective nonlinear coefficient d_{eff} . However, for MTSPS crystal, we may assume, as in NPP, that the influence of the d_{YXX} coefficient is predominant in the case of birefringence phase matching. Comparison of the expected ratio between the second harmonic intensities from MTSPS-phase I and NPP, respectively, could then lead to

$$\frac{I_{\text{MTSPS}}^{2\omega}}{I_{\text{NPP}}^{2\omega}} = \left(\frac{d_{YXX}^{\text{MTSPS}}}{d_{YXX}^{\text{NPP}}} \right)^2 = 3.0$$

This ratio is in reasonable agreement with the experimental one, 2.4, as deduced from a semi-quantitative SHG powder test. A similar estimation for MTSPS phase II (taking $d_{\text{eff}} = d_{YXX}$) leads to a calculated ratio equal to 1.4, also in good agreement with the experimental value of 1.3. Therefore, d_{IJK} estimates using the oriented gas model are in keeping with experimental powder test data, in spite of the fact that the results of these tests are only qualitative, and strongly depend on the granulometry of the powder. The d_{IJK} values calculated using the oriented gas model should furthermore provide a reasonable estimate of the d_{IJK} values of MTSPS crystals, the discrepancy with the actual ones being probably smaller than 15%, as exemplified by comparison with NPP related experimental data.

Conclusion

We have investigated the NLO properties of 4-substituted 4'-(*n*-sulfonatoalkyl)stilbazolium which are heterocyclic analogs of stilbenes. This approach has led to the discovery of two new active crystalline materials called MTSPS and SPS, both exhibiting large second-order optical nonlinear effects as pointed out by their SHG powder tests. The former is more efficient than NPP in its two hydrated crystal modifications. In both cases the water molecule is involved in a strong hydrogen bond network that plays a key role in the crystalline cohesion. This crystalline material is attractive for second harmonic generation from Nd³⁺:YAG operating at $1.06 \mu\text{m}$. The latter is interesting for blue light emission from semiconductor laser diodes operating around 820 nm.

Moreover these molecules possess a high molecular hyperpolarizability β , as shown by EFISHG measurements together with a large permanent dipole moment, which makes them potentially useful for inclusion in side-chain polymers followed by an orientation of the chromophore by electrical poling. These compounds also have hydrophilic and hydrophobic parts, especially those bearing a long alkyl chain (13); they could have potential interest in the preparation of Langmuir-Blodgett thin films. Furthermore, for the first time, the conformation of a 3-(sulfonatopropyl)stilbazolium group has been studied both computationally and by X-ray technique. Work is

(32) Sigelle, M.; Hierle, R. *J. Appl. Phys.* 1981, 52, 4199.

(33) Bosshard, C.; Sutter, K.; Schlessler, R.; Günter, P. *J. Opt. Soc. Am. B* 1993, 10, 867.

in progress to study the possible incorporation of these zwitterionic chromophores in various new NLO materials.

Experimental Section

Instrumentation. ^1H nuclear magnetic resonance (NMR) spectral data were obtained on a Bruker AC 200 spectrometer; chemical shifts (δ in ppm) are reported downfield from TMS. UV-vis spectra were recorded on a Shimadzu 2101PC spectrophotometer. IR spectra were taken on a Perkin-Elmer 21 spectrophotometer. Melting points were determined on a Reichert microscope with a Mettler FP 82 hot stage. Differential scanning calorimetry (DSC) curves were recorded on a Perkin-Elmer DSC2 and DSC 7 apparatus, with heating rate $10\text{ }^\circ\text{C}/\text{min}$.

Preparation of 4-Methyl-1-(*n*-sulfonatoalkyl)pyridinium (7, *n* = 3 or 4).¹⁰ *General Procedure.* 4-Picoline was treated at $0\text{ }^\circ\text{C}$ with 1 equiv of the appropriate alkanesultone (6), leading to crystalline 4-methyl-1-(*n*-sulfonatoalkyl)pyridinium (7), which was used for the subsequent reactions without further purification.

Preparation of 4-Methyl-1-(2-sulfonatoethyl)pyridinium (7, *n* = 2).¹² To 50 g (0.27 mol) of the sodium salt of isethionic acid were added 175 mL of SOCl_2 and 1 mL of DMF. The solution was heated under reflux for 3 h, then cooled to $40\text{ }^\circ\text{C}$, and reduced under vacuum. The remaining mixture is poured in 50 mL of water and extracted with ether. The organic layer was dried over sodium sulfate, reduced under vacuum, and distilled leading to a light yellow liquid of pure 2-chloroethanesulfonyl chloride (9, yield 54%). At $0\text{ }^\circ\text{C}$, 5 g (53.5 mmol) of 4-picoline in 50 mL of acetic acid was added slowly to 4.3 g (26 mmol) of the sulfonyl chloride 9. The mixture was stirred for 2 h at room temperature; then the solvent was removed under reduce pressure, leading to a black tar. Two recrystallizations from ether afforded pure 4-methyl-1-(2-sulfonatoethyl)pyridinium (7, *n* = 2) as a white hygroscopic powder. Mp $260\text{ }^\circ\text{C}$ (dec). Calcd for $\text{C}_8\text{H}_{11}\text{NO}_3\text{S}$: C, 47.75; H, 5.51; N, 6.96. Found: C, 47.61; H, 5.55; N, 6.86. ^1H NMR δ_{H} (200 MHz; solvent D_2O , internal lock acetone- d_6) 2.7 (3H, s); 3.6 (2H, t, $J = 7\text{ Hz}$); 4.90 (2H, t, $J = 7\text{ Hz}$); 7.9 (2H, d, $J = 8\text{ Hz}$); 8.8 (2H, d, $J = 8\text{ Hz}$).

Preparation of 4-Substituted 4'-(*n*-Sulfonatoalkyl)stilbazolium (2). *General Procedure.*¹⁰ To a solution of 7 in 15 mL of anhydrous ethanol was added 1 equiv of the arylaldehyde and a catalytic amount of pyrrolidine. The mixture was heated under reflux until reaction completion was shown by TLC (2–10 h) and then cooled to $0\text{ }^\circ\text{C}$. The precipitated product was filtered and washed with pentane. Recrystallization from aqueous ethanol afforded pure 4-substituted 4'-(*n*-sulfonatoalkyl)stilbazolium, 2.

Preparation of 4-(Methylthio)-4'-(3-sulfonatopropyl)stilbazolium (MTSPS) (10). MTSPS was prepared as above in 78% yield. Recrystallization from aqueous ethanol (2/1) afforded pure 10 as yellow needles (MTSPS-phase I). Mp decomposition at $300\text{ }^\circ\text{C}$. Calcd for $\text{C}_{17}\text{H}_{19}\text{NO}_3\text{S}_2\cdot\text{H}_2\text{O}$: C, 55.56; H, 5.76; N, 3.81; O, 17.42; S 17.45. Found: C, 55.62; H, 5.47; N, 3.81; S, 17.43; O, 17.39. Recrystallization from aqueous ethanol (2/1), containing 1 equiv of pyrrolidine relative to the amount of product in solution, afforded pure 10 as yellow orange plates (MTSPS-phase II). Calcd for $\text{C}_{17}\text{H}_{19}\text{NO}_3\text{S}_2\cdot\text{H}_2\text{O}$: C, 55.56; H, 5.76; N, 3.81; O, 17.42; S 17.45. Found: C, 55.82; H, 5.86; N, 3.73; O, 17.39; S, 17.05. Heating phase II crystals at $200\text{ }^\circ\text{C}$ for 1 h gave the phase III as an orange powder.

Calcd for $\text{C}_{17}\text{H}_{19}\text{NO}_3\text{S}_2$: C, 58.42; H, 5.47; N, 4.01; S, 18.35; O, 13.75. Found: C, 58.44; H, 5.44; N, 3.87; S, 18.37; O, 14.15. ^1H NMR δ_{H} (200 MHz; solvent DMSO- d_6) 2.2 (2H, quint, $J = 6\text{ Hz}$); 2.45 (2H, t, $J = 6\text{ Hz}$); 2.45 (3H, s); 4.6 (2H, t, $J = 6\text{ Hz}$); 7.35 (2H, d, $J = 10\text{ Hz}$); 7.45 (1H, d, $J = 17\text{ Hz}$); 7.65 (2H, d, $J = 10\text{ Hz}$); 7.95 (1H, d, $J = 17\text{ Hz}$); 8.2 (2H, d, $J = 8\text{ Hz}$); 8.9 (2H, d, $J = 8\text{ Hz}$).

Preparation of 4-Butyl-4'-(3-sulfonatopropyl)stilbazolium (BSPS) (11). The product was prepared in 71% yield. Recrystallization from ethanol afforded pure 11 as a nearly white powder. Mp $280\text{ }^\circ\text{C}$ (dec). Calcd for $\text{C}_{20}\text{H}_{25}\text{NO}_3\text{S}\cdot\text{H}_2\text{O}$: C, 63.63; H, 7.21; N, 3.71. Found: C, 63.41; H, 7.32; N, 3.64. ^1H NMR δ_{H} (200 MHz; solvent DMSO- d_6) 0.85 (3H, t, $J = 6\text{ Hz}$); 1.25 (2H, sext, $J = 6\text{ Hz}$); 1.6 (2H, quint, $J = 6\text{ Hz}$); 2.2 (2H, t, $J = 7\text{ Hz}$); 2.4 (2H, t, $J = 7\text{ Hz}$); 2.6 (2H, t, $J = 6\text{ Hz}$); 4.6 (2H, t, 6 Hz); 7.35 (2H, d, $J = 9\text{ Hz}$); 7.45 (1H, d, $J = 15\text{ Hz}$); 7.7 (2H, d, $J = 9\text{ Hz}$); 7.9 (2H, d, $J = 15\text{ Hz}$); 8.25 (2H, d, $J = 9\text{ Hz}$); 8.9 (2H, d, $J = 9\text{ Hz}$).

Preparation of 4'-(3-Sulfonatopropyl)stilbazolium (SPS) (12). The same procedure as above was used. Recrystallization of the crude product from aqueous ethanol (2/1) afforded pure 12 (SPS-phase I) as straw-colored needles. Decomposition at $280\text{ }^\circ\text{C}$. Calcd for $\text{C}_{16}\text{H}_{17}\text{SNO}_3\cdot\text{H}_2\text{O}$: C, 59.80; H, 5.96; N, 4.36. Found: C, 59.89; H, 5.91; N, 4.41. Recrystallization of the crude product from aqueous ethanol (2/1) containing 1 equiv of pyrrolidine afforded pure 12 as colorless plates (SPS-phase II). Decomposition around $280\text{ }^\circ\text{C}$. Calcd for $\text{C}_{16}\text{H}_{17}\text{NO}_3\text{S}\cdot 2\text{H}_2\text{O}$: C, 56.62; H 6.24; N, 4.13. Found: C, 56.40; H, 6.15; N, 4.01. Heating phase I at $140\text{ }^\circ\text{C}$ for 1 h afforded phase III. Calcd for $\text{C}_{16}\text{H}_{17}\text{NO}_3\text{S}$ C, 63.35; H, 5.65; N:4.62. Found: C 62.61; H 5.76; N, 4.36. ^1H NMR δ_{H} (200 MHz; solvent DMSO- d_6) 2.25 (2H, quint, $J = 7\text{ Hz}$); 2.45 (2H, t, $J = 7\text{ Hz}$); 4.65 (2H, t, $J = 7\text{ Hz}$); 7.5 (4H, m); 7.75 (2H, m); 8 (1H, d, $J = 18\text{ Hz}$); 8.25 (2H, d, $J = 8\text{ Hz}$); 8.95 (2H, d, $J = 8\text{ Hz}$).

Preparation of 4-(Decylthio)-4'-(3-sulfonatopropyl)stilbazolium (13). The compound was prepared in 71% yield according to the general procedure. Recrystallization from ethanol afforded pure 13 as yellow product. Mp $250\text{ }^\circ\text{C}$ (dec). Calcd for $\text{C}_{26}\text{H}_{37}\text{NO}_3\text{S}_2\cdot 2\text{H}_2\text{O}$: C, 61.02; H, 8.08; N, 2.74. Found: C, 60.90; H, 7.57; N, 2.56. ^1H NMR δ_{H} (200 MHz; solvent DMSO- d_6) 0.8 (3H, t, $J = 6\text{ Hz}$); 1.1–1.5 (m, 14H); 1.6 (m, 2H); 2.2 (2H, quint, $J = 6\text{ Hz}$); 2.4 (2H, t, $J = 7\text{ Hz}$); 3 (2H, t, $J = 8\text{ Hz}$); 4.6 (2H, t, $J = 7\text{ Hz}$); 7.35 (2H, d, $J = 9\text{ Hz}$); 7.45 (1H, d, $J = 16\text{ Hz}$); 7.65 (2H, d, $J = 9\text{ Hz}$); 7.95 (1H, d, $J = 16\text{ Hz}$); 8.15 (2H, d, $J = 9\text{ Hz}$); 8.9 (2H, d, $J = 9\text{ Hz}$).

Preparation of 3,5-Di-*tert*-butyl-4'-(3-sulfonatopropyl)stilbazolium (14). The compound was prepared in 69% yield. Recrystallization from ethanol afforded pure 14. Mp $>300\text{ }^\circ\text{C}$. Calcd for $\text{C}_{24}\text{H}_{33}\text{NO}_3\text{S}\cdot\text{H}_2\text{O}$: C, 66.48; H, 8.14; N, 3.23. Found: C, 66.59; H, 8.21; N, 3.11. ^1H NMR δ_{H} (200 MHz; solvent CD_3OD) 1.4 (18H, s); 2.5 (2H, quint, $J = 8\text{ Hz}$); 2.85 (2H, t, $J = 8\text{ Hz}$); 4.85 (2H, t, $J = 8\text{ Hz}$); 7.5 (1H, d, $J = 16\text{ Hz}$); 7.65 (3H, m); 8.1 (1H, d, $J = 16\text{ Hz}$); 8.25 (2H, d, $J = 9\text{ Hz}$); 8.9 (2H, d, $J = 9\text{ Hz}$).

Molecular Hyperpolarizability Measurements (β). For β measurements, we have used the electric-field-induced second-harmonic (EFISH) generation technique, based on the wedge fringe method in analogy with the classical “maker fringes” method. The fundamental beam is emitted by a Q-switched, mode-locked Nd^{3+} :YAG laser operating at $1.34\text{ }\mu\text{m}$, and generating pulse trains (repeti-

tion rate 10 Hz) where the individual pulse duration is around 160 ps, and the global envelope of the train is 90 ns. The beam is polarized vertically and focused into the cell (typical focal distance 40 cm, corresponding to a peak intensity around 500 MW C m⁻²). The visible light is filtered out using a Schott RG 1000 filter. High-voltage pulses of up to 10 kV amplitude and 2 μ s duration are applied synchronously to the laser pulses, so that the electric field has a large known value inside the liquid and is oriented parallel to the electric laser field. The interelectrode distance is 2 mm. The cell is translated transversally by using a stepping motor (1 step = 0.1 μ m). A combination of a KG5 and an OG 610 Schott filters is used to filter out the output beam; neutral densities filters can be used to avoid saturation of the photomultiplier. The signal is averaged, and the amplitude of the second harmonic power is recorded as a function of time, for several solutions of different concentrations of the molecule to be measured. Each measurement is referenced, at the beginning of each run, to the harmonic signal from the pure solvent. The results are reported in Table 7.

X-ray Experimental Section. A single crystal of MTSPS-phase I (10) was cut out from a cluster of crystals and mounted on a rotation-free goniometer head. A systematic search in reciprocal space using a Philips PW1100/16 automatic diffractometer showed that crystals of MTSPS-phase I belong to monoclinic system.

Quantitative data were obtained at -100 °C achieved using a local-build gas flow device. All experimental parameters used are given in Table 1. The resulting data set was transferred to a VAX computer, and for all subsequent calculations the Enraf-Nonius SDP/VAX package³⁴ was used with the exception of a local data reduction program. Three standard reflections measured every hour during the entire data collection period showed

no significant trend. The raw step-can data were converted to intensities using the Lehmann-Larsen method³⁵ and then corrected for Lorentz and polarized factors.

The structure was solved using Multan.³⁶ After refinement of the heavy atoms, a difference-Fourier map revealed maximas of residual electronic density close to the positions expected for hydrogen atoms; they were introduced in structure factor calculations with isotropic temperature factors such as $B(H) = 1.3 B \text{ eqv}(C) \text{ \AA}^2$ but not refined. The absolute configuration given by Multan was checked by comparing x, y, z and $-x, -y, -z$ refinements. At this stage empirical absorption corrections were applied using the method of Walker and Stuart³⁷ since face indexation was not possible under the cold gas stream. Full least-squares refinements: $\sigma^2(F^2) = \sigma^2_{\text{counts}} + (pI)^2$. A final difference map revealed no significant maxima: + 0.18/-0.15 e \AA^{-3} . The scattering factor coefficients and anomalous dispersion coefficients come respectively from ref 38.

Acknowledgment. C.S. thanks the CNET and the CNRS for a cofinanced BDI fellowship. France-Telecom is gratefully acknowledged for financial support of this work under Contract 88-6B 007909245. We thank M. Barzoukas and A. Fort for the use of their laser setup for the SHG powder tests. Many thanks also to the US Naval Research Laboratory in Washington (Washington, DC) for partial financial support of this work under US Navy Grant 00014-90-J-2011.

Supplementary Material Available: Tables of temperature factors for anisotropic atoms and hydrogen atom positions (2 pages); observed and calculated structure factors amplitudes ($\times 10$) for all observed reflections (7 pages). Ordering information is given on any current masthead page.

(35) Lehman, M. S.; Larsen, F. K. *Acta Crystallogr.* 1974, A30, 580.

(36) Germain, G.; Main, P.; Woolfson, M. M. *Acta Crystallogr.* 1971, A27, 368.

(37) Walker, N.; Stuart, D. *Acta Crystallogr.* 1983, A39, 158.

(38) Cromer, D. T.; Waber, J. T. *Int. Tables X-ray Crystallogr.* 1974, 4, The Kynoch Press, Birmingham: (a) Table 2.2b; (b) Table 2.3.1.

(34) Frenz, B. A. The Enraf-Nonius CAD4-SDP. In *Computing in Crystallography*; Schenk, H., Olthof-Hazekamp, R., Van Koningveld, H., Bassi, G.C., Eds.; Delft University Press: Delft, 1978; pp 64-71.